Electronic Supplementary Information

Observation of *bcc*-like framework in polyhydrido copper nanoclusters

Qi-Lin Guo,[a,‡] Bao-Liang Han,[b,‡] Cun-Fa Sun,[a,‡] Zhi Wang,[b] Yunwen Tao,[*,c] Jin-Qing Lin,[a] Geng-Geng Luo,[*,a] Chen-Ho Tung,[b] and Di Sun[*,b]

Experimental Details

$Cu(CF_3CO_2)_2{\cdot}H_2O$, $Cu(CH_3CO_2)_2{\cdot}H_2O$, 1,3-bis(diphenylphosphino)propane (dppp), 1,2-bis(diphenylphosphino)ethane (dppe), (4-isopropyl)thiophenol ($^{i}PrC_6H_4SH$), cyclohexanethiol (ChSH), *tert*-butylthiol ($^{t}BuSH$), 2-thiophenethiol, 4-*tert*-butylbenzenethiol ($^{t}BuPhSH$), 4-*tert*-butylbenzylmercaptan ($^{t}BuPhCH_2SH$), tetrahydrofuran-d_8, sodium borodeuteride ($NaBD_4$), were purchased from Energy Chemical Reagent Co. Ltd. (Shanghai, China). Sodium borohydride ($NaBH_4$), dichloromethane (CH_2Cl_2), methanol, tetrahydrofuran, ethanol, ethyl ether, and *n*-hexane were purchased from Sinopharm Chemical Reagent Co. Ltd. (Shanghai, China). All reagents were used as received without further purification.

Synthesis of $[Cu_{28}H_{16}(ChS)_4(dppp)_4(CF_3CO_2)_8]$ (1): 28.9 mg $Cu(CF_3CO_2)_2{\cdot}H_2O$ in 1 mL methanol solution and 15 mg 1,3-bis (diphenylphosphino)propane (dppp) propane in 0.5 mL dichloromethane solution were added After 30 min, 1.22 μL cyclohexanethiol in 0.5 mL dichloromethane solution was added. After 30 min, methanol solution of $NaBH_4$ (7 mg/mL) was added dropwise under vigorous stirring. After aging at room temperature for 6h, the organic phase was washed with distilled water several times to remove the organic phase, dissolved in dichloromethane and centrifuged at 8000 r/min for 3 min. By diffusing *n*-hexane at room temperature for several days, red crystals suitable for X-ray diffraction study was obtained. Yield: ~15% (based on Cu). IR (KBr pellet, cm^{-1}): 3419 (w), 3053 (w), 2918 (w), 2850 (w), 1652 (s), 1576 (w), 1485 (w), 1436 (s), 1408 (w), 1335 (w), 1258 (w), 1194 (s), 1139 (m), 1099 (w), 1027 (w), 995 (w), 961 (w), 937 (w), 888 (w), 842 (m), 788 (w), 742 (w), 725 (s), 691 (s), 662 (w), 549 (w), 509 (s), 480 (w), 453 (w).

Synthesis of $[Cu_{28}D_{16}(ChS)_4(dppp)_4(CF_3CO_2)_8]$ ($\mathbf{1_D}$). The synthesis procedure of $\mathbf{1_D}$ is identical to that of **1** except that $NaBD_4$ was used instead of

$NaBH_4$.

Synthesis of $[Cu_{28}H_{16}(dppe)_4(^iPrC_6H_4S)_4(CH_3CO_2)_6Cl_2]$ (2): 20 mg of $Cu(OAc)_2 \cdot H_2O$ and 10 mg of 1,2-bis(diphenylphosphino)ethane (dppe) were dissolved in a mixed solvent of 1 mL ethanol and 4 mL dichloromethane, followed by the addition of 3 μL of (4-isopropyl)thiophenol ($^iPrC_6H_4SH$) under vigorous stirring. After 15 min stirring, 1 mL ethanol solution containing 10 mg $NaBH_4$ (0.265 mmol) was added dropwise under vigorous stirring (1200 rpm). The reaction was aged for 8 h at room temperature during vigorous stirring, and the solution changed from green to deep red. Then, the solution was filtrated and stored at room temperature, from which the red block crystals were formed within one week. Yield: ~67% (based on copper). IR (KBr pellet, cm^{-1}): 3406 (w), 3053 (w), 2961 (w), 2916 (w), 2347 (m), 2329 (m), 1554 (m), 1488 (w), 1412 (s), 1337 (w), 1179 (w), 1100 (w), 1011 (w), 918 (w), 817 (m), 733 (m), 690 (s), 663 (m), 610 (w), 513 (m).

Synthesis of $[Cu_{28}D_{16}(dppe)_4(^iPrC_6H_4S)_4(CH_3CO_2)_6Cl_2]$ ($\mathbf{2_D}$). The synthesis procedure of $\mathbf{2_D}$ is identical to that of **2** except that $NaBD_4$ was used instead of $NaBH_4$.

Synthesis of $[Cu_{28}H_{16}(^tBuS)_4(dppp)_4(CF_3CO_2)_8]$ (3) and $[Cu_{28}H_{16}(TpS)_4(dppp)_4(CF_3CO_2)_8]$ (4): Clusters **3** and **4** were synthesized by a similar procedure with **1**, except that the *tert*-butylthiol and 2-thiophenethiol instead of cyclohexanethiol. The red block crystals were isolated. Yield: 10% for **3** and 11% for **4**. IR (KBr pellet, cm^{-1}) for **3**: 3419 (w), 3057 (w), 2955 (w), 2923 (w), 2861 (w), 1650 (s), 1573 (w), 1485 (w), 1435 (m), 1308 (w), 1193 (s), 1142 (m), 1127 (m), 1100 (w), 1099 (w), 1026 (w), 998 (w), 969 (w), 935 (w), 842 (m), 787 (w), 742 (w), 725 (s), 691 (s), 654 (w), 547 (w), 509 (s), 479 (m). IR (KBr pellet, cm^{-1}) for **4**: 457 (w), 3056 (w), 2976 (w), 2908 (w), 2849 (w), 1644 (s), 1485 (w), 1435 (m), 1396 (w), 1195 (s), 1136 (m), 1040 (m), 1032 (w), 1001 (w), 969 (w), 933 (w), 844 (m), 789 (w), 727 (s), 686 (s), 556 (w), 511 (s), 470 (w).

Synthesis of $[Cu_{28}H_{16}(dppe)_4(^tBuPhS)_4(CH_3CO_2)_6Cl_2]$ (5) and $[Cu_{28}H_{16}(dppe)_4(^tBuPhCH_2S)_4(CH_3CO_2)_6Cl_2]$ (6): Clusters **5** and **6** were synthesized by a similar procedure with **2**, except that the 4-*tert*-butylbenzenethiol and 4-*tert*-butylbenzylmercaptan instead of (4-isopropyl)thiophenol. The red rod-shaped and block crystals were isolated. Yield: 57% for **5** and 71% for **6**. IR (KBr pellet, cm^{-1}) for **5**: 3057 (w), 2961 (w), 2898 (w), 2352 (m), 1562 (m), 1483 (w), 1412 (s), 1262 (w), 1100 (w), 1007 (w), 822 (w), 742 (m), 689 (s), 658 (m), 610 (w), 543 (w), 513 (s). IR (KBr pellet, cm^{-1}) for **6**: 3053 (w), 2956 (w), 2903 (w), 2347 (s), 1558 (m), 1479 (w), 1408 (s), 1267 (w), 1187 (w), 1104 (w), 1064 (w), 1025 (w), 822 (w), 742 (m), 694 (s), 658 (m), 557 (w), 513 (s).

Single-crystal X-ray structure determination

Single crystals of **1**-**6** with appropriate dimensions was chosen under an optical microscope and quickly coated with high vacuum grease (Dow Corning Corporation). Intensity diffraction data was collected at 173 K for **1**, **3**, **4**, **5** and 100 K for **2**, **6** on a Rigaku Oxford Diffraction XtaLAB system Synergy diffractometer equipped with a HyPix-6000HE area detector, using a Cu Kα radiation (λ = 1.54184 Å) from PhotonJet micro-focus X-ray source. The diffraction images were processed and scaled using the CrysAlisPro software.[S1] The structures were solved using the charge-flipping algorithm, as implemented in the program SUPERFLIP[S2] and refined by full-matrix least-squares techniques against F_o^2 using the SHELXL program[S3] through the OLEX2 interface.[S4] Hydrogen atoms at carbon were placed in calculated positions and refined isotropically by using a riding model. Appropriate restraints or constraints were applied to the geometry and atomic displacement parameters of the atoms in the cluster. All structures were examined using the Addsym subroutine of PLATON[S5] to ensure that no additional symmetry could be applied to the models.

Physical measurement

UV-vis absorption spectra were recorded on a PerkinElmer Lambda 1050 UV-vis spectrophotometer. Emission spectra were measured on a Hitachi F-7000 spectrometer. FT-IR spectra were recorded on a Thermo Scientific Nicolet iS50 FTIR Spectrometer. Electrochemical measurements were performed at room temperature in a three-electrode system on a potentiostat (CHI760E) under N_2: a glass carbon electrode was selected as the working electrode, and the Pt electrode and saturated calomel electrode (SCE) served as the counter and reference electrodes. ^1H NMR spectra were recorded on a Bruker AVANCE III 500 MHz spectrometer. ^2H NMR spectra were recorded on a Bruker AVANCE III 850 MHz spectrometer. X-ray photoelectron spectroscopy (XPS) measurements were performed on a Kratos Axis Ultra DLD spectrometer with a monochromatic Al Kα X-ray source. Binding energies were referred to the C 1s peak of adventitious carbon at 284.8 eV. Morphology of the sample and elemental composition analyse were measured using an SU-8010 field emission scanning electron microscope (FESEM; Hitachi Ltd., Tokyo, Japan) equipped with an Oxford-Horiba Inca XMax50 energy dispersive X-ray spectroscopy (EDS) attachment (Oxford Instrument Analytical, High Wycombe, England). High-resolution mass spectra (HR-MS) were recorded on a Bruker impact II high definition mass spectrometer equipped with the quadrupole and time-of-flight (Q-TOF) modules in the positive ion mode. Typical measurement conditions are as follows: end plate offset = 500 V; dry gas = 3 L/min, nebulizer = 0.3 bar, capillary voltage = 6000 V, spray temperature = 100 °C; sample flow rate = 180 μL/h; collision gas, N_2. The data analyses of mass spectra were performed based on the isotope distribution patterns using Bruker Compass Data Analysis software 4.4 SR1 (Version 4.4). The reported *m/z* values represent the monoisotopic mass of the most abundant peak within the isotope pattern. Thermogravimetric analysis (TGA) was measured on a

Mettler-Toledo TGA/DSC3+ instrument at the heating rate of 10 °C/min in a nitrogen atmosphere.

Computational methods

Full geometry optimizations of **1** and **2** was performed by density functional theory (DFT) calculations using the ORCA 4.0 version program package[S6] with the BP86 functional[S7] and the all-electron Def2-SV(P) set from EMSL Basis Set Exchange Library.[S8] The input coordinates were obtained from the X-ray single crystal structure data. Their optimized geometries were characterized as a minimum by vibrational analysis.

Table S1-S6 & Fig. S1-Fig. S18

Table S1. Crystal data and structure refinement for $[Cu_{28}H_{16}(ChS)_4(CF_3COO)_8(dppp)_4•CH_2Cl_2]$ ($1•CH_2Cl_2$).

Identification code	$Cu_{28}H_{16}(dppp)_4(ChS)_4(CF_3CO_2)_8·CH_2Cl_2$
Empirical Formula	$C_{149}H_{166}Cu_{28}O_{16}F_{24}P_8S_4Cl_2$
Temperature / K	173.00(10)
Crystal system	monoclinic
Space group	*C*2/*c*
a / Å	34.5054(5)
b / Å	17.4137(2)
c / Å	33.4531(5)
α / °	90
β / °	118.640(2)
γ / °	90
Volume / $Å^3$	17641.5(5)
Z	4
ρ_{calcg} / cm^3	1.843
μ/mm^{-1}	5.598
F(000)	9737
Crystal size/mm^3	0.1 × 0.08 × 0.05
Radiation	CuKα (λ = 1.54184)
2θ range for data collection / °	5.836 to 133.196
Index ranges	$-41 \le h \le 37$, $-20 \le k \le 8$, $-39 \le l \le 39$
Reflections collected	48374
Independent reflections	15334 [R_{int} = 0.0341, R_{sigma} = 0.0344]
Data/restraints/parameters	15334/38/1115
Goodness-of-fit on F^2	1.029
Final R indexes [I>=2σ (I)]	R_1 = 0.0488, wR_2 = 0.1336
Final R indexes [all data]	R_1 = 0.0576, wR_2 = 0.1388
Largest diff. peak/hole / e $Å^{-3}$	2.38/–1.73

Table S2. Crystal data and structure refinement for [$Cu_{28}H_{16}$(dppe)$_4$(^{i}PrC_6H_4S)$_4$(CH_3CO_2)$_6$$Cl_2$] (2).

Identification code	$Cu_{28}H_{16}$(dppe)$_4$(^{i}PrC_6H_4S)$_4$(CH_3CO_2)$_6Cl_2$
Empirical Formula	$C_{152}H_{174}Cl_2Cu_{28}O_{12}P_8S_4$
Temperature / K	100.00(10)
Crystal system	monoclinic
Space group	*P*2$_1$/*c*
a / Å	18.6379(3)
b / Å	25.8870(5)
c / Å	17.9828(4)
α / °	90
β / °	108.318(2)
γ / °	90
Volume / Å^3	8236.7(3)
Z	2
ρ_{calcg} / cm^3	1.782
μ/mm^{-1}	5.682
F(000)	4424.0
Crystal size/mm^3	0.05 × 0.04 × 0.02
Radiation	CuKα (λ = 1.54184)
2θ range for data collection / °	6.05 to 149.006
Index ranges	$-23 \le h \le 19$, $-30 \le k \le 32$, $-22 \le l \le 21$
Reflections collected	63959
Independent reflections	16616 [R_{int} = 0.0469, R_{sigma} = 0.0425]
Data/restraints/parameters	16616/701/1598
Goodness-of-fit on F^2	1.029
Final R indexes [I>=2σ (I)]	R_1 = 0.0432, wR_2 = 0.1011
Final R indexes [all data]	R_1 = 0.0560, wR_2 = 0.1079
Largest diff. peak/hole / e Å^{-3}	0.71/-0.97

Table S3. Crystal data and structure refinement for [$\mathrm{Cu_{28}H_{16}(dppp)_4(^{\mathit{t}}BuS)_4(CF_3CO_2)_8}$] (3).

Identification code	$\mathrm{Cu_{28}H_{16}(dppp)_4(^{\mathit{t}}BuS)_4(CF_3CO_2)_8}$
Empirical Formula	$\mathrm{C_{140}H_{156}Cu_{28}O_{16}F_{24}P_8S_4}$
Temperature / K	173.00(10)
Crystal system	monoclinic
Space group	*C*2/*m*
a / Å	21.3652(7)
b / Å	28.1638(9)
c / Å	17.7736(6)
α / °	90
β / °	100.122(3)
γ / °	90
Volume / $Å^3$	10528.4(6)
Z	2
ρ_{calcg} / cm^3	1.484
μ/mm^{-1}	4.437
F(000)	4672.0
Crystal size/mm^3	0.08 × 0.04 × 0.03
Radiation	CuKα (λ = 1.54184)
2θ range for data collection / °	7.78 to 154.172
Index ranges	$-25 \le h \le 25$, $-33 \le k \le 19$, $-21 \le l \le 21$
Reflections collected	32368
Independent reflections	9437 [R_{int} = 0.0614, R_{sigma} = 0.0486]
Data/restraints/parameters	9437/197/593
Goodness-of-fit on F^2	0.996
Final R indexes [I>=2σ (I)]	R_1 = 0. 0753, wR_2 = 0. 2146
Final R indexes [all data]	R_1 = 0.0875, wR_2 = 0.2294
Largest diff. peak/hole / e $Å^{-3}$	2.90/-1.08

Table S4. Crystal data and structure refinement for $[Cu_{28}H_{16}(dppp)_4(TpS)_4(CF_3CO_2)_8]$ (4).

Identification code	$Cu_{28}H_{16}(dppp)_4(TpS)_4(CF_3CO_2)_8$
Empirical Formula	$C_{140}H_{132}Cu_{28}O_{16}F_{24}P_8S_8$
Temperature / K	173.00(10)
Crystal system	orthorhombic
Space group	*Pbca*
a / Å	28.1238(7)
b / Å	22.3309(4)
c / Å	27.2663(5)
α / °	90
β / °	90
γ / °	90
Volume / Å^3	17124.0(6)
Z	4
ρ_{calcg} / cm^3	1.866
μ/mm^{-1}	5.920
F(000)	9504.0
Crystal size/mm^3	0.10 × 0.08 × 0.07
Radiation	CuKα (λ = 1.54184)
2θ range for data collection / °	6.286 to 154.974
Index ranges	$-24 \le h \le 33$, $-12 \le k \le 26$, $-32 \le l \le 30$
Reflections collected	55110
Independent reflections	15132 [R_{int} = 0.0460, R_{sigma} = 0.0422]
Data/restraints/parameters	15132/1161/1458
Goodness-of-fit on F^2	1.047
Final R indexes [I>=2σ (I)]	R_1 = 0. 0960, wR_2 = 0. 2607
Final R indexes [all data]	R_1 = 0.1145, wR_2 = 0.2786
Largest diff. peak/hole / e Å^{-3}	2.45/-3.23

Table S5. Crystal data and structure refinement for $[Cu_{28}H_{16}(dppe)_4(^{t}BuPhS)_4(CH_3CO_2)_6Cl_2]$ (5).

Identification code	$Cu_{28}H_{16}(dppe)_4(^{t}BuPhS)_4(CH_3CO_2)_6Cl_2$
Empirical Formula	$C_{156}H_{182}Cl_2Cu_{28}O_{12}P_8S_4$
Temperature / K	173.00(10)
Crystal system	triclinic
Space group	*P*-1
a / Å	17.5118(6)
b / Å	17.6946(7)
c / Å	18.7236(7)
α / °	97.227(3)
β / °	104.392(3)
γ / °	115.803(4)
Volume / Å^3	4873.9(4)
Z	1
ρ_{calcg} / cm^3	1.525
μ/mm^{-1}	4.808
F(000)	2244.0
Crystal size/mm^3	0.06 × 0.05 × 0.03
Radiation	CuKα (λ = 1.54184)
Index ranges	$-20 \leq h \leq 20$, $-21 \leq k \leq 18$, $-22 \leq l \leq 21$
Reflections collected	51074
Independent reflections	17177 [R_{int} = 0.0461, R_{sigma} = 0.0483]
Data/restraints/parameters	17177/579/1303
Goodness-of-fit on F^2	1.068
Final R indexes [I>=2σ (I)]	R_1 = 0. 0457, wR_2 = 0. 1299
Final R indexes [all data]	R_1 = 0.0550, wR_2 = 0.1371
Largest diff. peak/hole / e Å^{-3}	2.02/-0.91

Table S6. Crystal data and structure refinement for [$Cu_{28}H_{16}(dppe)_4(^tBuPhCH_2S)_4(CH_3CO_2)_6Cl_2$] (6).

Identification code	$Cu_{28}H_{16}(dppe)_4(^tBuPhCH_2S)_4(CH_3CO_2)_6Cl_2$
Empirical Formula	$C_{160}H_{190}Cl_2Cu_{28}O_{12}P_8S_4$
Temperature / K	100.00(10)
Crystal system	monoclinic
Space group	$P2_1/c$
a / Å	17.9266(6)
b / Å	31.7028(7)
c / Å	18.1745(6)
α / °	90
β / °	113.215(4)
γ / °	90
Volume / $Å^3$	9492.7(6)
Z	2
ρ_{calcg} / cm^3	1.585
μ/mm^{-1}	3.248
F(000)	4552.0
Crystal size/mm^3	0.05 × 0.045 × 0.02
Radiation	CuKα (λ = 1.54184)
Index ranges	$-23 \leq h \leq 23$, $-42 \leq k \leq 39$, $-22 \leq l \leq 24$
Reflections collected	80703
Independent reflections	23333 [R_{int} = 0.0411, R_{sigma} = 0.0459]
Data/restraints/parameters	23333/486/1476
Goodness-of-fit on F^2	1.035
Final R indexes [I>=2σ (I)]	R_1 = 0.0414, wR_2 = 0. 0880
Final R indexes [all data]	R_1 = 0.0612, wR_2 = 0.0941
Largest diff. peak/hole / e $Å^{-3}$	1.74/-0.59

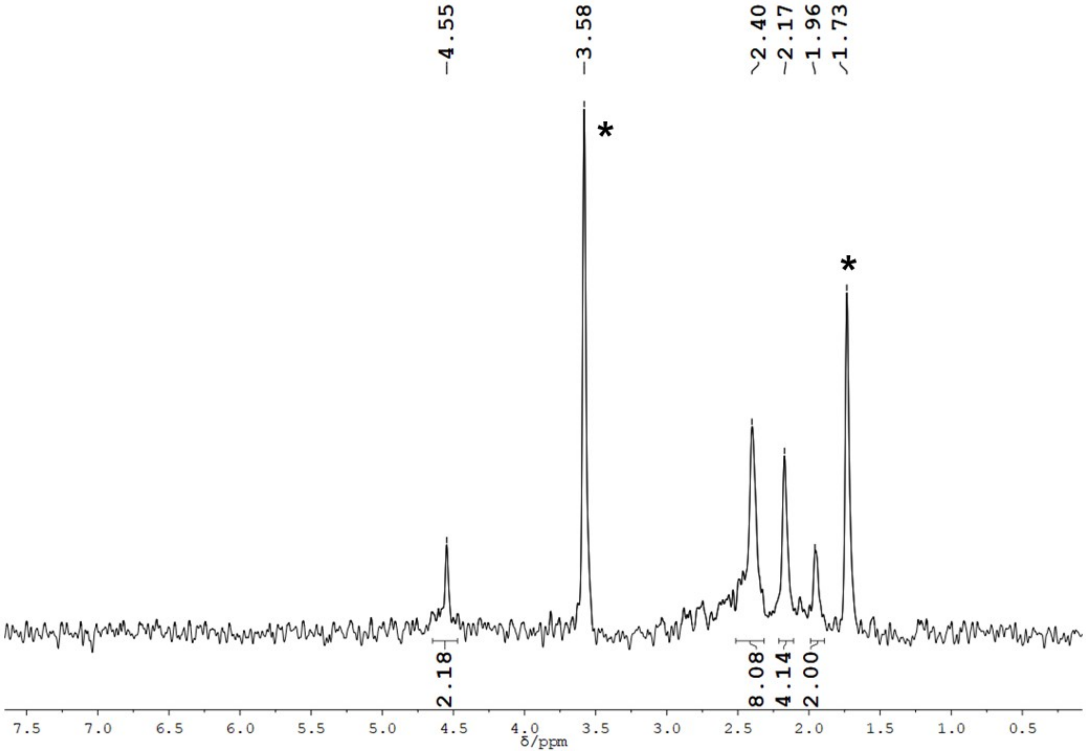

Fig. S1. ^{2}H-NMR spectrum of cluster $\mathbf{1_D}$ in THF. Note: * = THF-d_8.

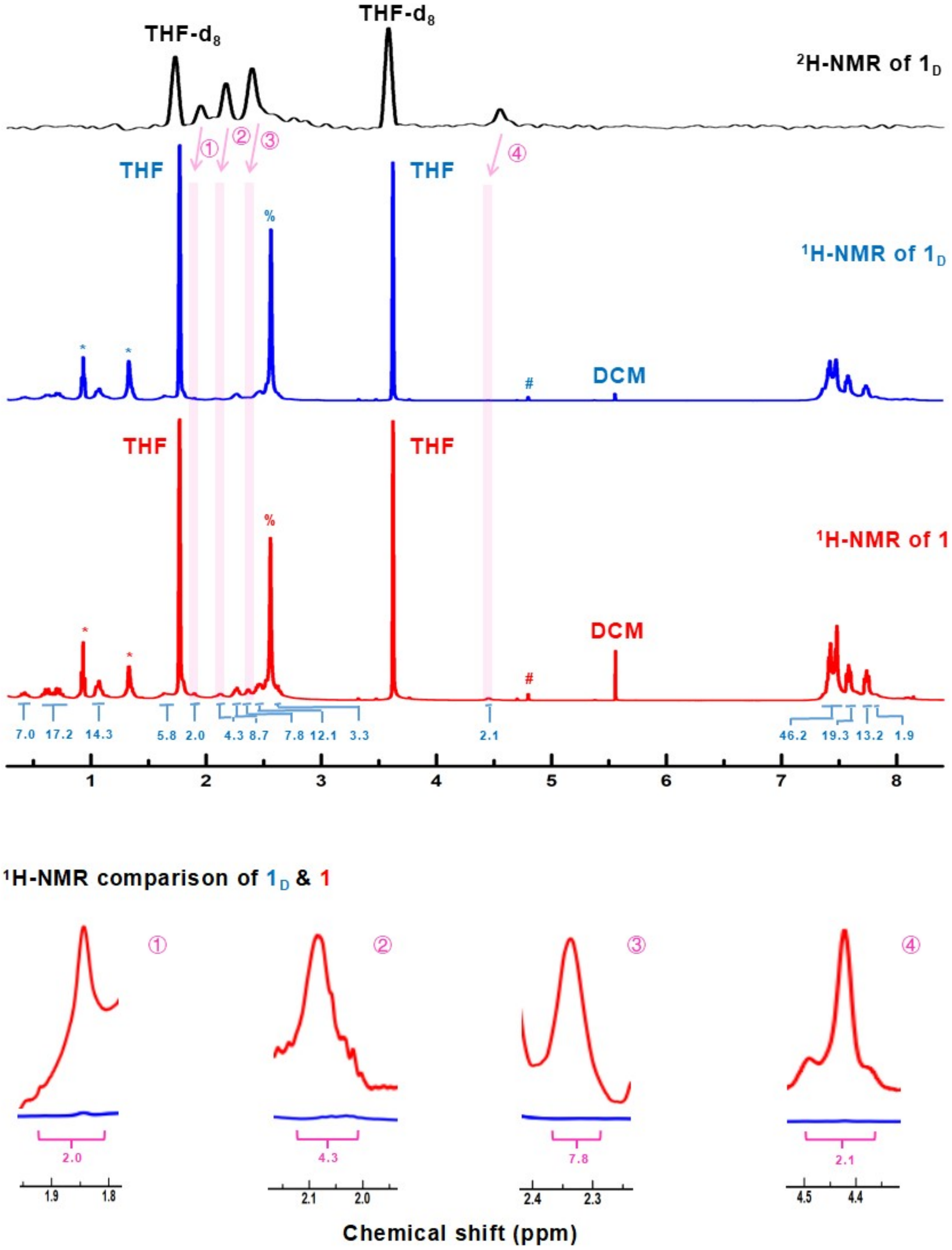

Fig. S2. ^{1}H-NMR comparison of **1_D** & **1**: near the shifts of **D**s, extra peaks appear respectively in the ^{1}H-NMR of **1** contrast to **1_D**, indicating the sixteen **H**s. Note: *, n-hexane; #, H_2； %, H_2O;.

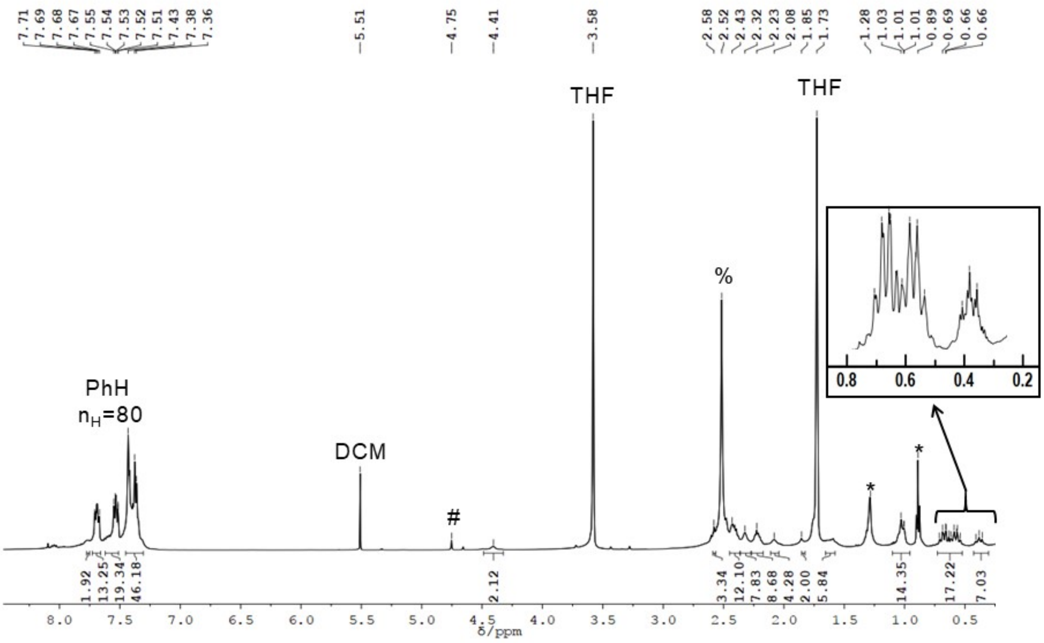

Fig. S3. ^{1}H-NMR spectrum **1** in THF-d_8. Note: *, *n*-hexane; %, H_2O; #, H_2.

Comments on NMR: In Fig. S4, the detailed ^{1}H-NMR spectrum of **1** are shown. The peaks at δ = 1.9, 2.1, 2.3, and 4.4 are attributed to the hydrides, while other peaks in the range of 0.5 to 5.5 ppm correspond to cyclohexanethiols and methylene protons of dppp The phenyl protons of dppp ligands local in 7.2 to 7.9 ppm. In addition, the extra impurities of solvents (dichloromethane, water, and *n*-hexane) were also detected.

.

A)

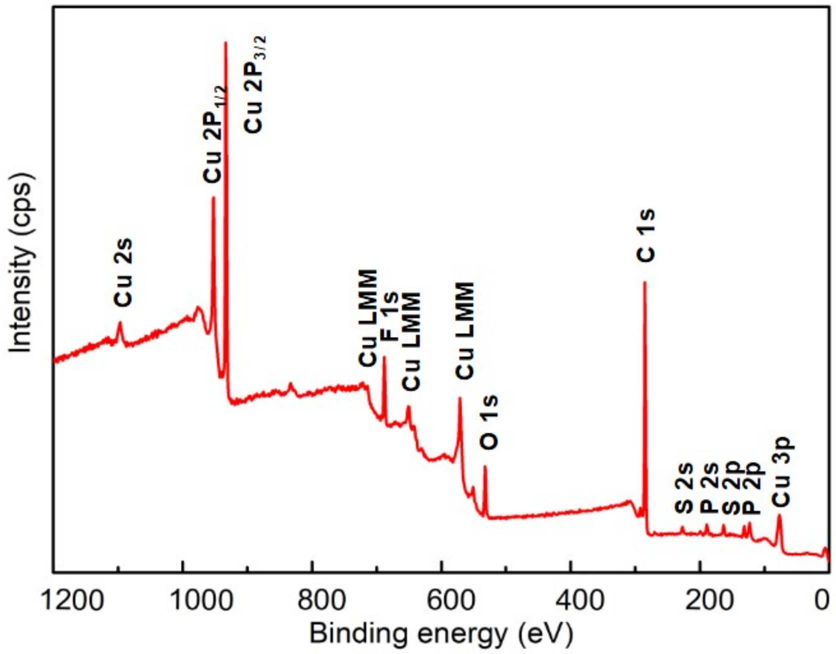

B)

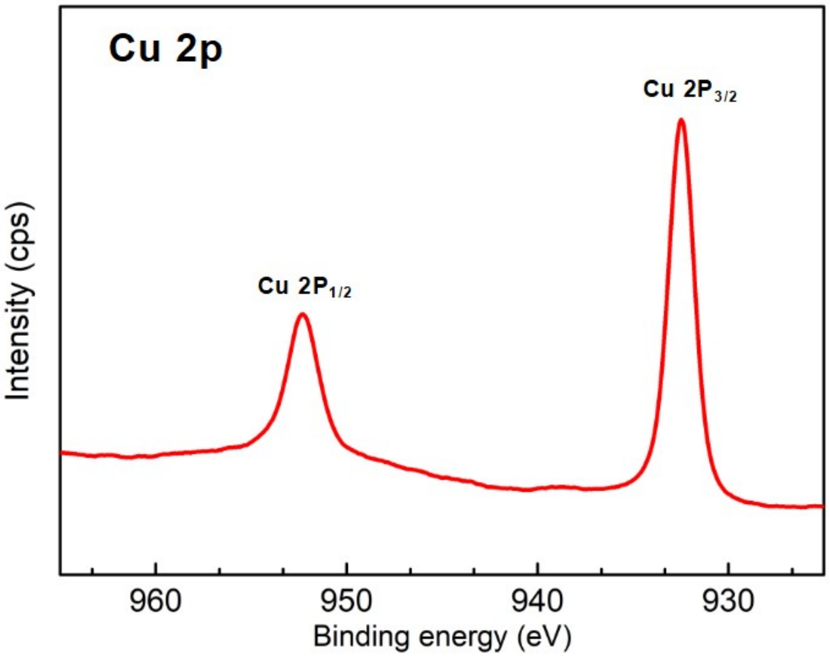

Fig. S4. A) The wide XPS spectrum of **1**. B) High-resolution XPS spectra of Cu 2p level of **1**.

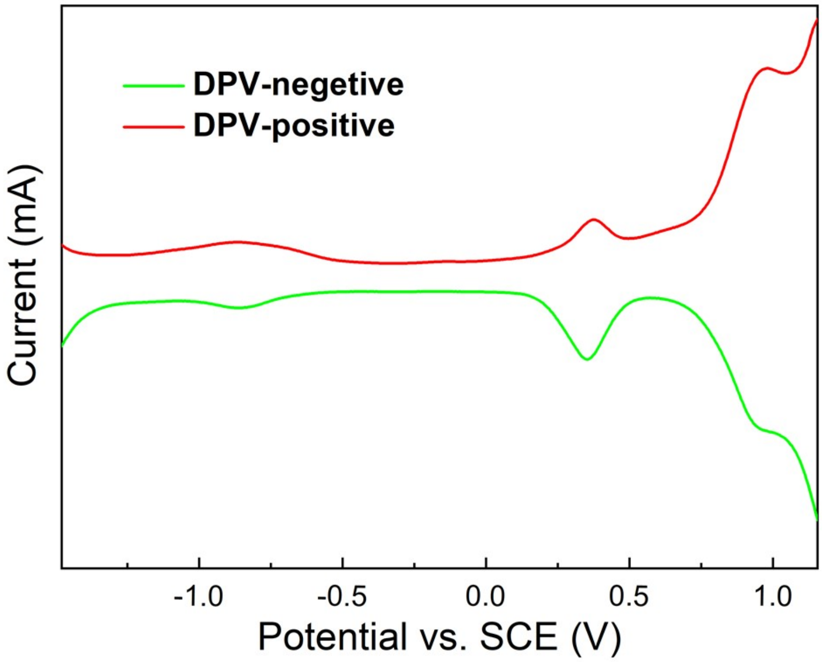

Fig. S5. DPV of **1** in 0.1 M $TBAPF_6/CH_2Cl_2$ at a scan rate 0.1 V/s under N_2 atmosphere.

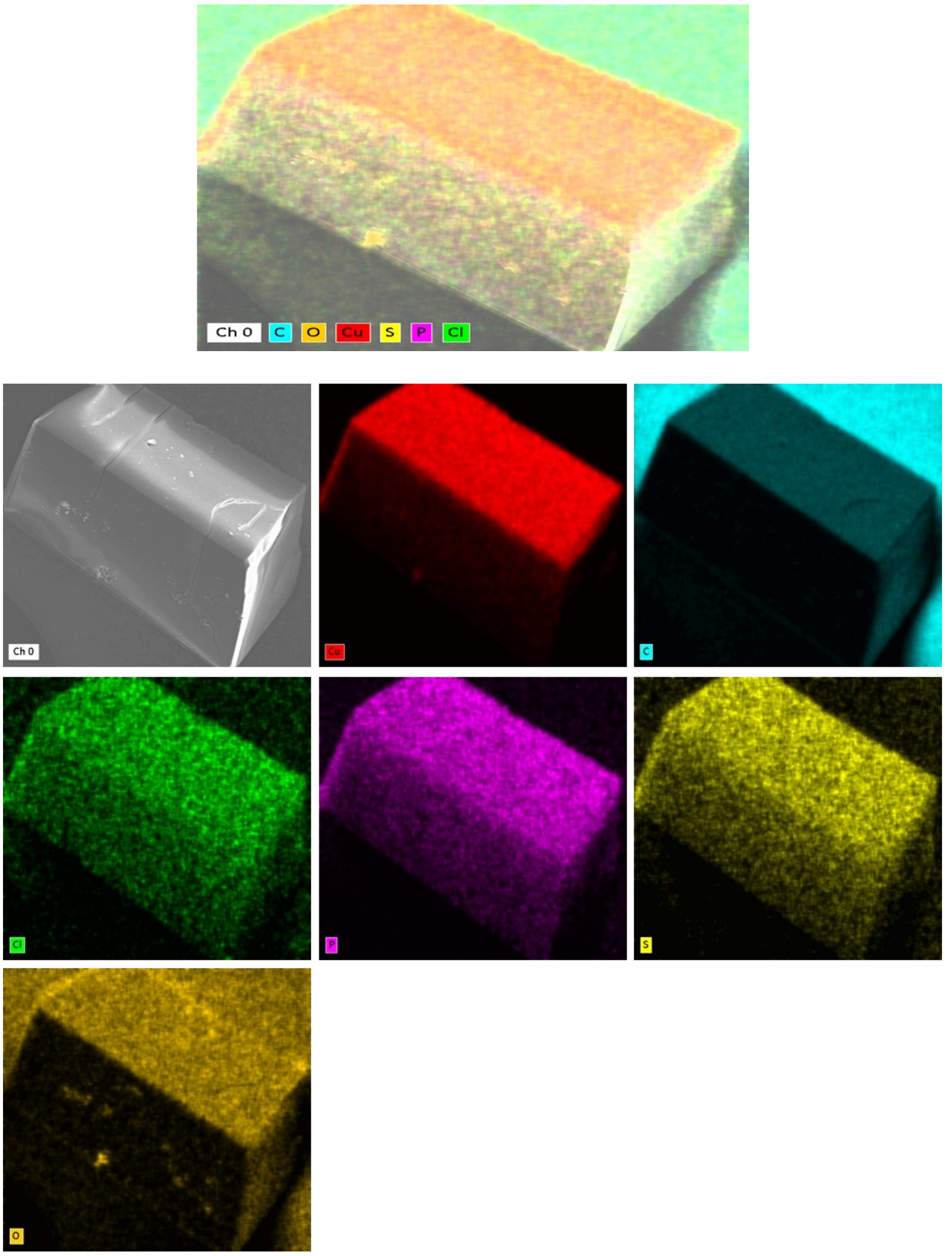

Fig. S6. The energy-dispersive X-ray spectroscopy survey spectrum of the cluster **2**.

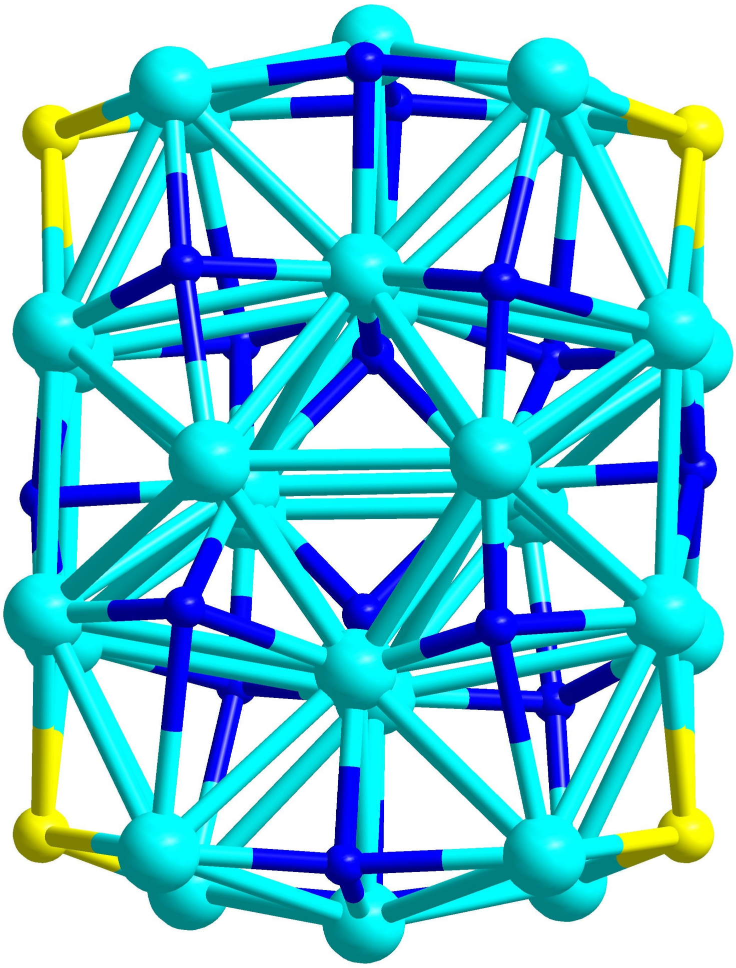

Fig. S7. The coordination environments of the 16 hydrides in **2**. Colour legend: Turquoise, Cu; Yellow, S; Blue, H.

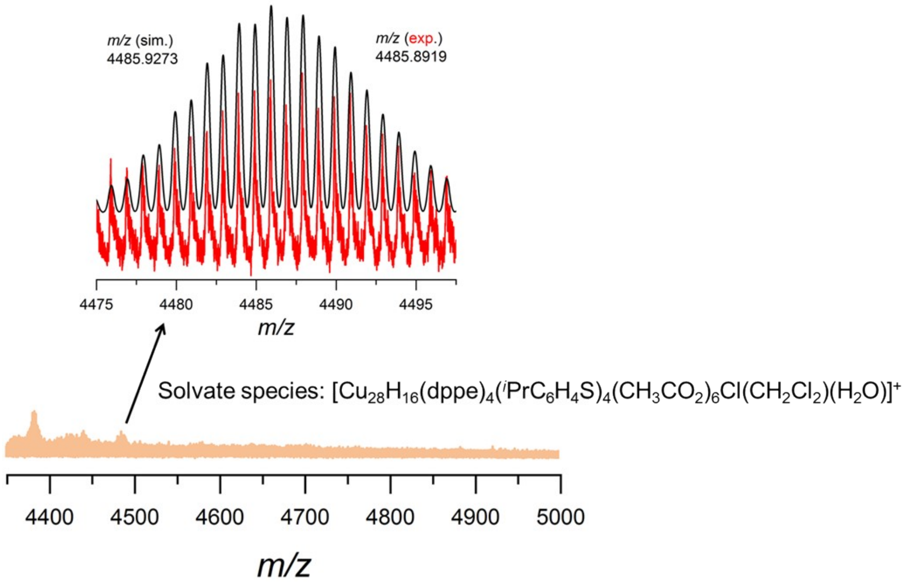

Fig. S8. The solvate species in positive-ion ESI-MS spectra of **2**.

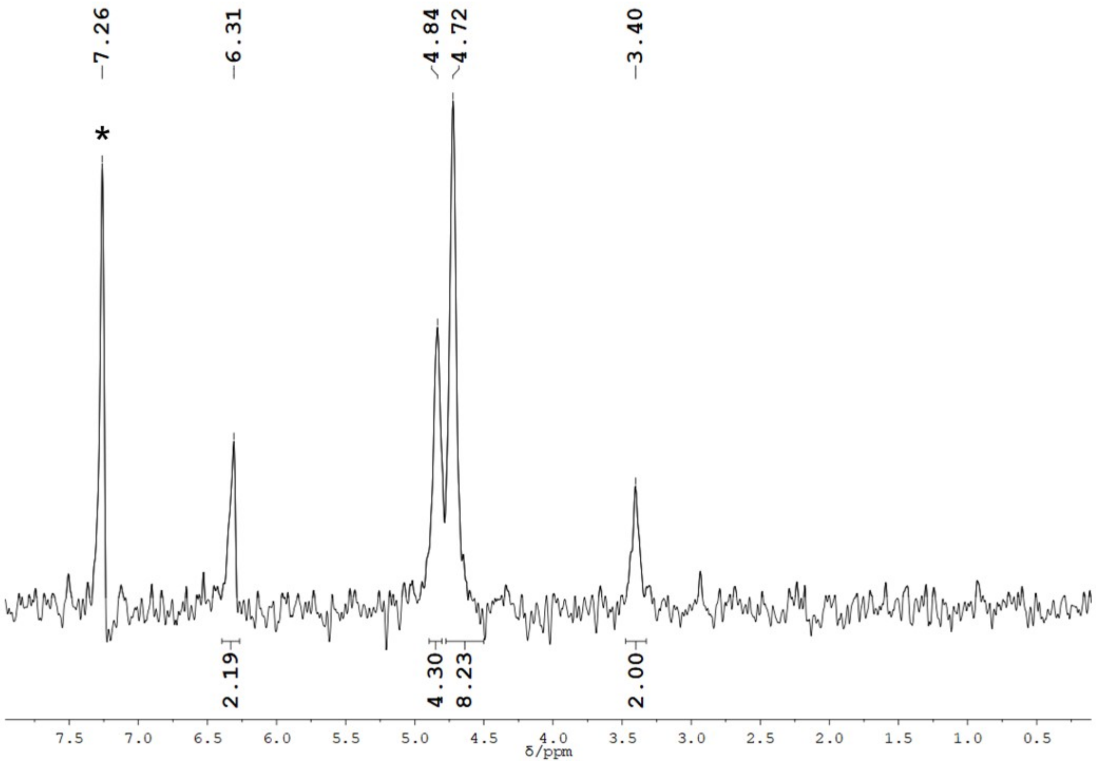

Fig. S9. ^{2}H-NMR spectrum of $\mathbf{2_D}$ in $CHCl_3$ (Note: * = $CDCl_3$).

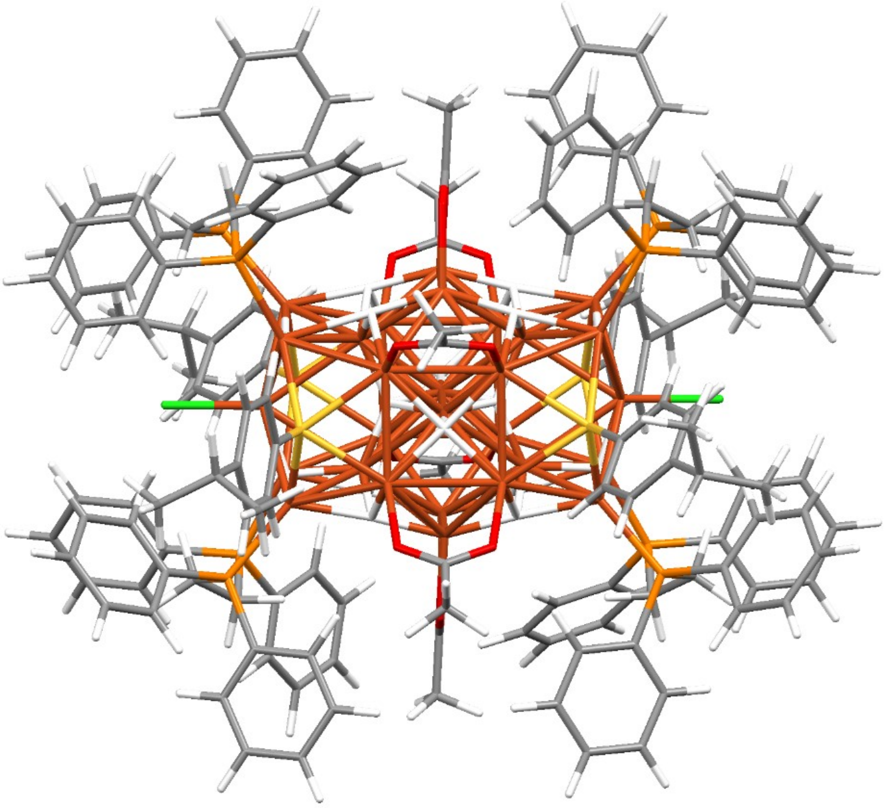

Fig. S10. DFT-Optimized structure of **2**. Atom colors: Cu brown; S yellow; P orange; C gray; O red; Cl green; H white.

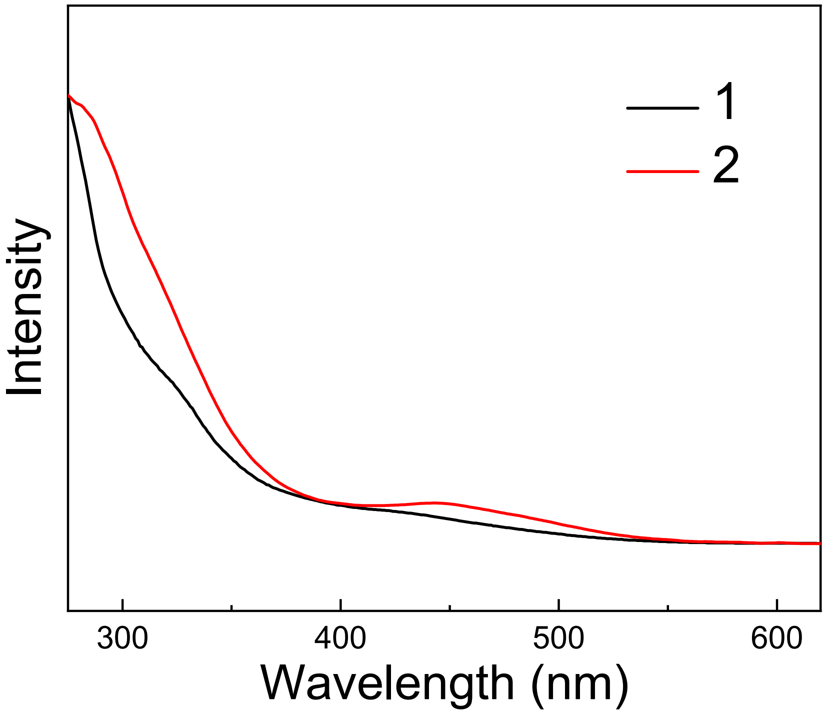

Fig. S11. UV/Vis absorption spectra of **1** and **2** in CH_2Cl_2 at room temperature.

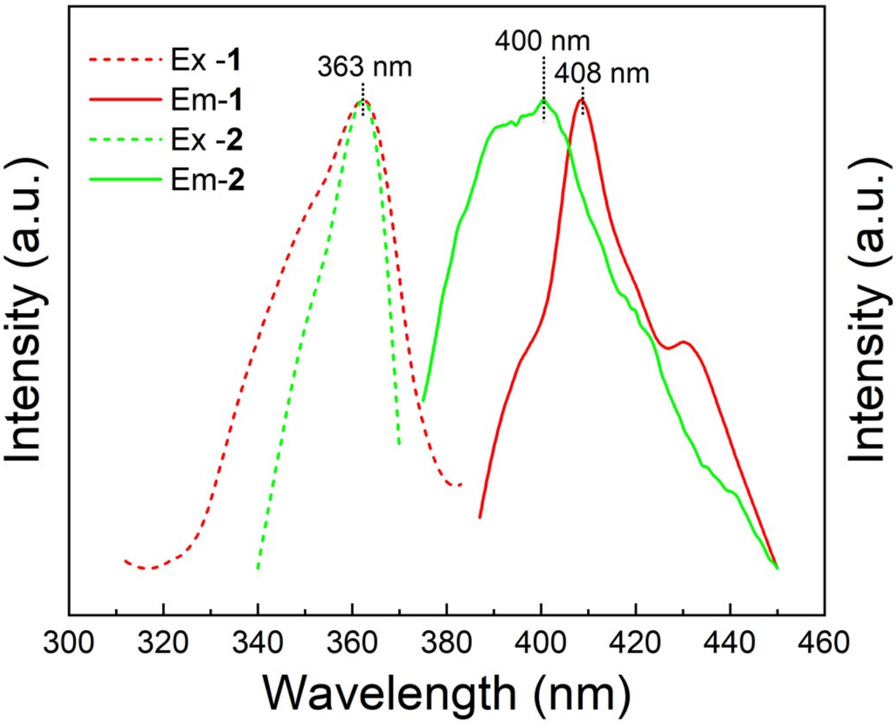

Fig. S12. Emission spectra of **1** and **2** in CH_2Cl_2 at room temperature.

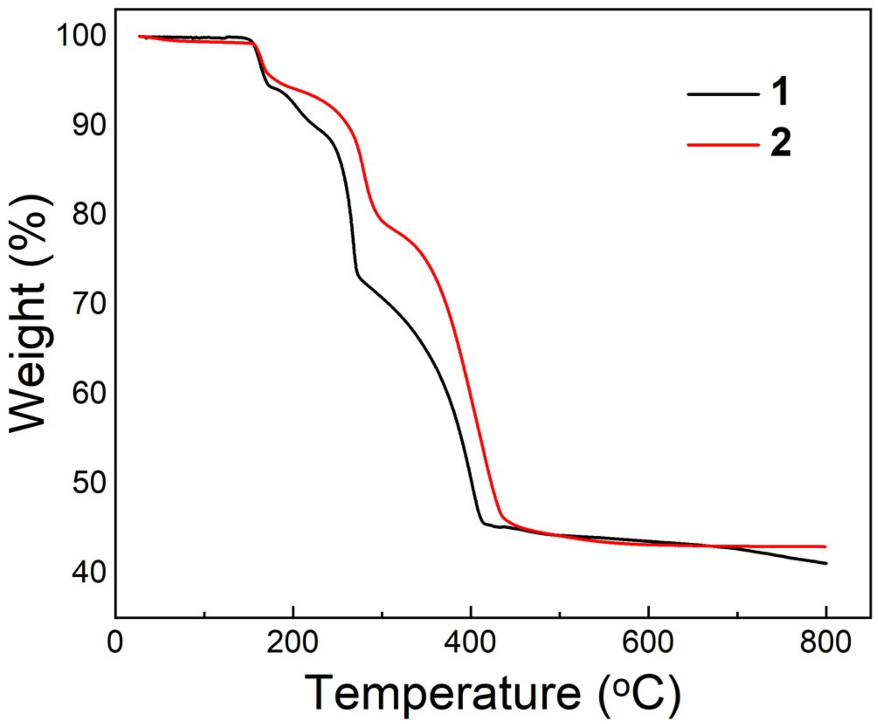

Fig. S13. TGA of **1** and **2** in a N_2 atmosphere.

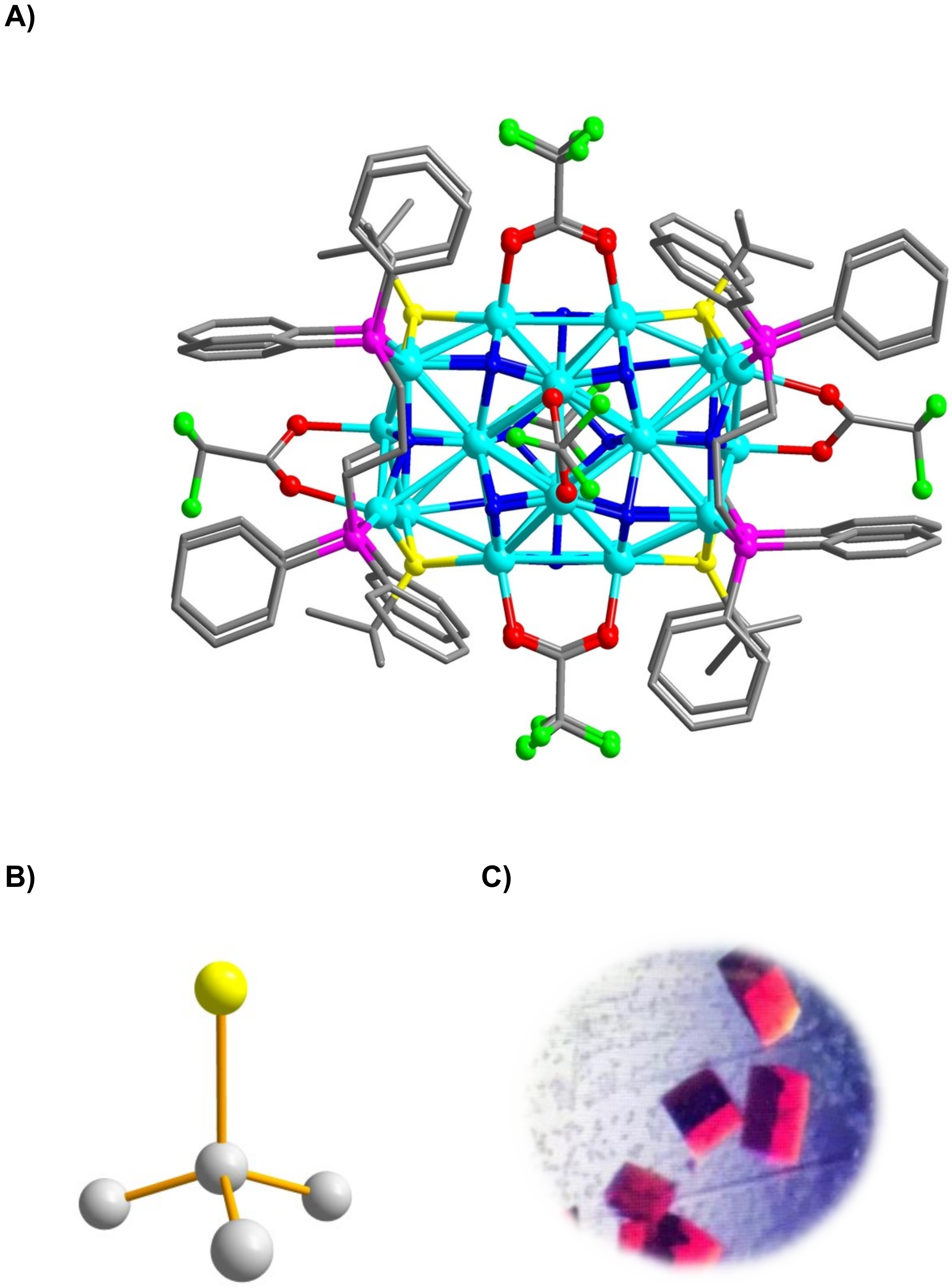

Fig. S14. (A) Molecular structure of **3** revealed by SC-XRD analysis. Turquoise: Cu; Pink: P; Yellow: S; Gray: C; Red: O; Green: F; Blue: H. CH_2Cl_2 solvents and H atoms located on carbon atoms are omitted for clarity. (B) Molecular structure of *tert*-butylthiol ligand. Hydrogen atoms omitted for clarity. (C) Optical microscopy image of crystals **3**.

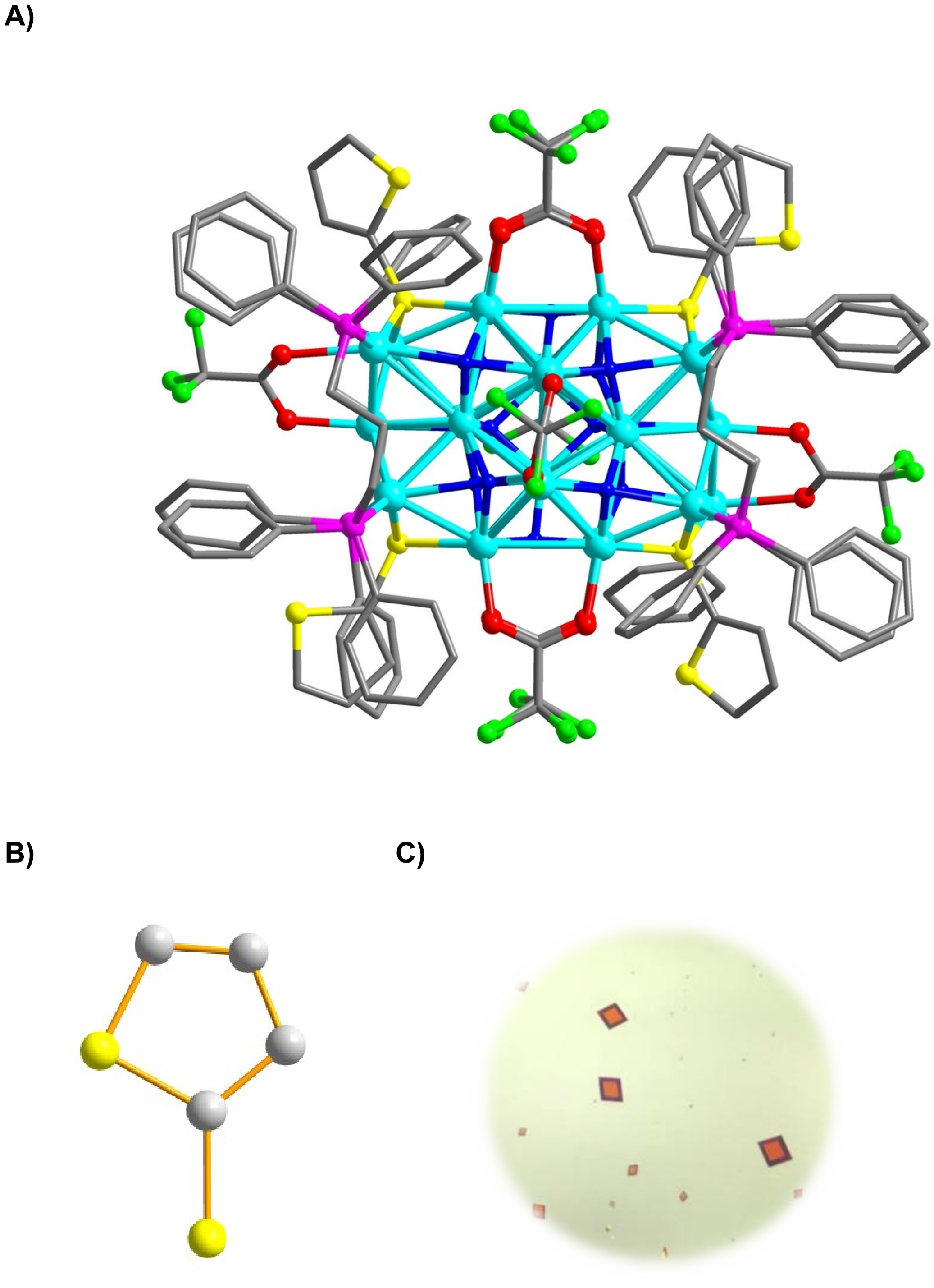

Fig. S15. Molecular structure of **4** revealed by SC-XRD analysis. Turquoise: Cu; Pink: P; Yellow: S; Gray: C; Red: O; Green: F; Blue: H. CH_2Cl_2 solvents and H atoms located on carbon atoms are omitted for clarity. (B) Molecular structure of 2-thiophenethiol. Hydrogen atoms omitted for clarity. (C) Optical microscopy image of crystals **4**.

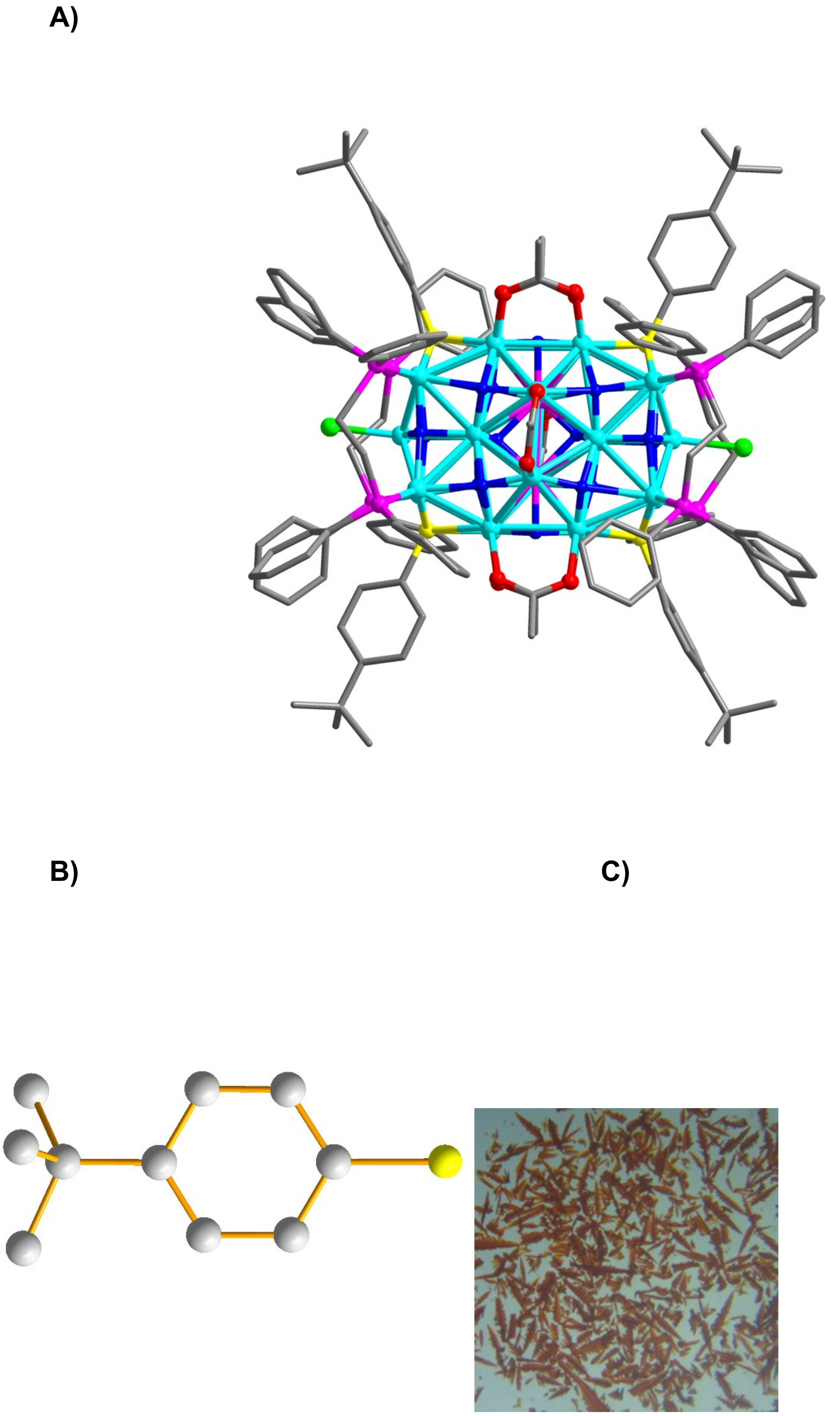

Fig. S16. (A) Molecular structure of **5** revealed by SC-XRD analysis. Orange: Cu; Pink: P; Yellow: S; Gray: C; Red: O; Green: Cl; Blue: H. H atoms located on carbon atoms are omitted for clarity. (B) Molecular structure of 4-*tert*-

butylbenzenethiol ligand. Hydrogen atoms omitted for clarity. (C) Optical microscopy image of crystals **5**.

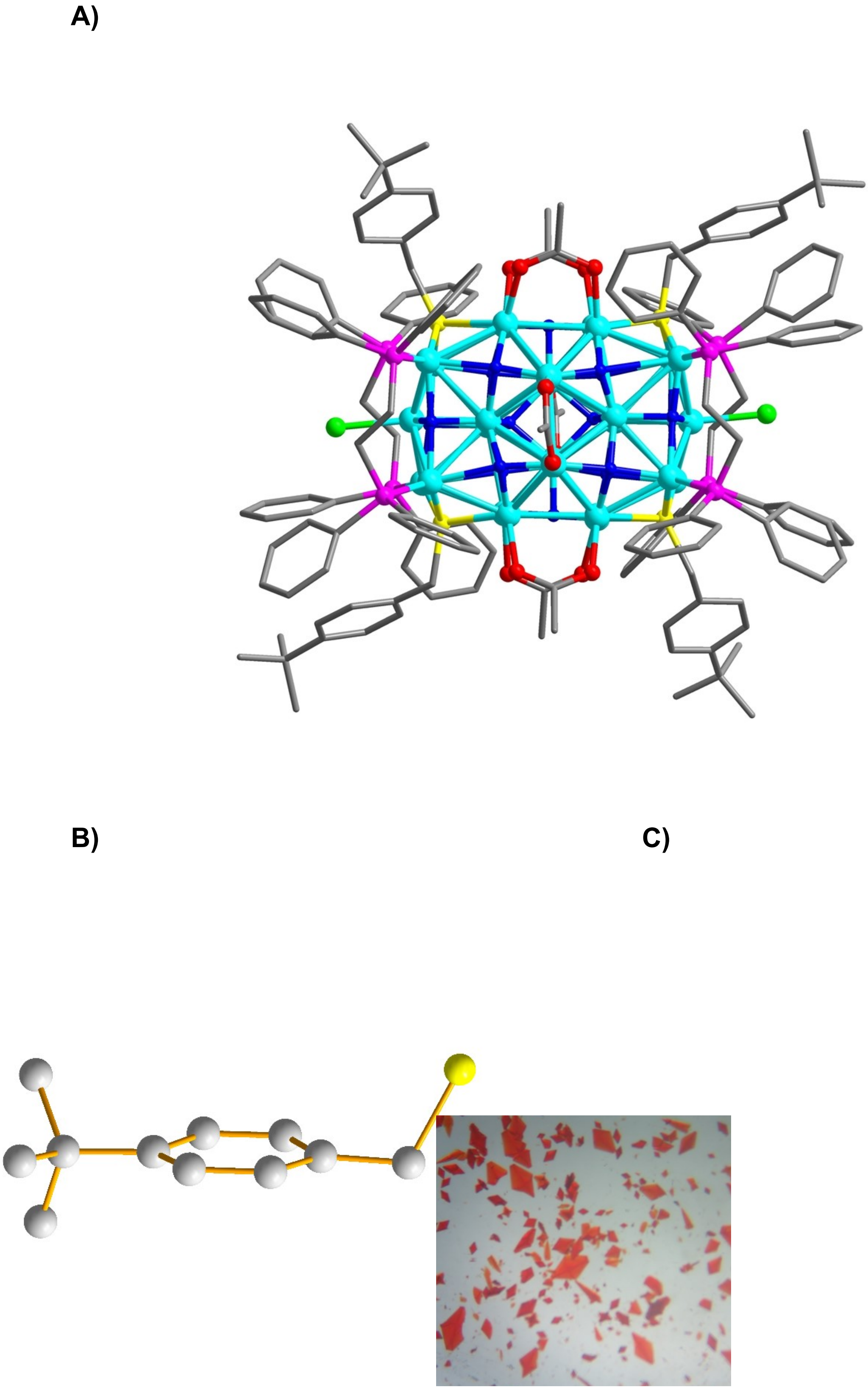

Fig. S17. (A) Molecular structure of **6** revealed by SC-XRD analysis. Turquoise: Cu; Pink: P; Yellow: S; Gray: C; Red: O; Green: Cl; Blue: H. H atoms located on carbon atoms are omitted for clarity. (B) Molecular structure of 4-*tert*-butylbenzylmercaptan ligand. Hydrogen atoms omitted for clarity. (C) Optical microscopy image of crystals **6**.

A)

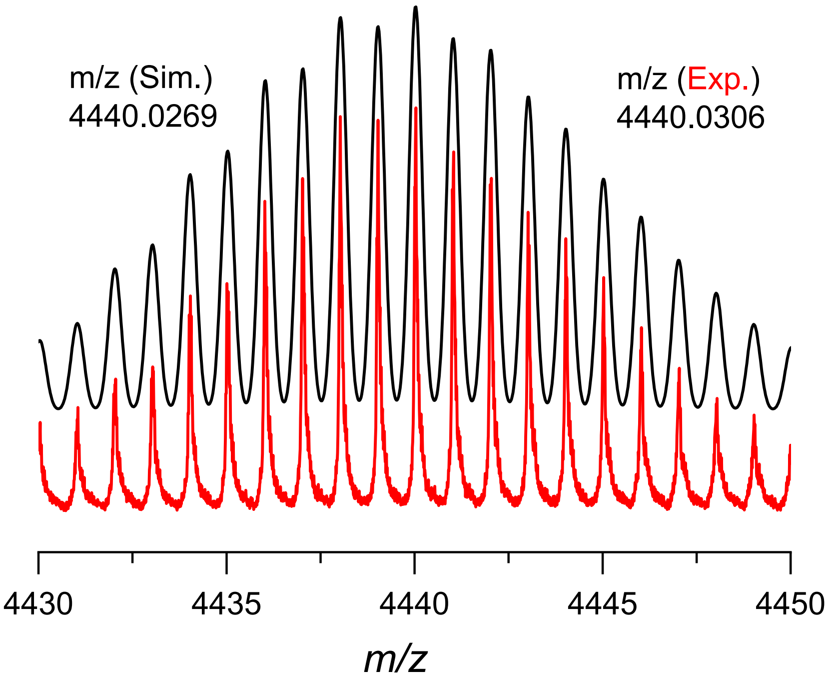

B)

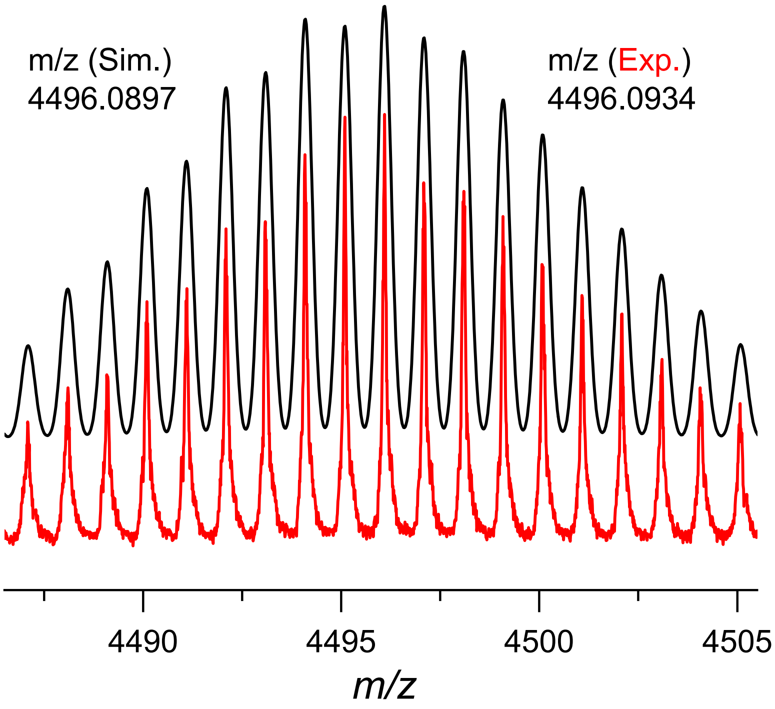

Fig. S18. Positive-ion ESI-MS spectra of **5** (A) and **6** (B) dissolved in CH_2Cl_2.

Supplementary references

[S1] CrysAlisPro, Rigaku OD, The Woodlands, TX, 2015.

[S2] L. Palatinus and G. Chapuis, *J. Appl. Crystallogr*., **2007**, 40, 786.

[S3] G. M. Sheldrick, *Acta. Crystallogr., Sect. C*., **2015**, 71, 3-8.

[S4] O. V. Dolomanov, L. J. Bourhis, R. J. Gildea, J. A. K. Howard and H. Puschmann, *J. Appl. Crystallogr.,* **2009**, 42, 339-341.

[S5] A. L. Spek, *Acta. Crystallogr., Sect. D*., **2009**, *61*, 148-155.

[S6] F. Neese, ORCA, version 4.2.0, Software update: the ORCA program system, version 4.0, WIREs Comput Mol Sci, 2017, 8, e1327.

[S7] a) A. D. Becke, *Phys. Rev. A* **1988**, 38, 3098-3100; b) J. P. Perdew, *Phys. Rev. B* **1986**, 33, 8822.

[S8] F. Weigend and R. Ahlrichs, *Phys. Chem. Chem. Phys*. **2005**, 7, 3297.